

Two-dimensional Imaging of Sizes and Number Densities of Nanoscaled Particles

H. Geitlinger, T. Streibel, R. Suntz and H. Bockhorn
Institut für Chemische Technik/Engler-Bunte-
Institut, Bereich Verbrennungstechnik,
Universität Karlsruhe (TH),
Kaiserstr.12, D-76128 Karlsruhe, Germany

Phone Number: ++49-721-608-2120
FAX Number: ++49-721-608-4820
E-mail: bockhorn@ict.uni-karlsruhe.de

ABSTRACT

In this work, a recently developed optical measurement technique for nonintrusive in-situ detection of two-dimensional fields of soot volume fractions, particle number densities and mean particle radii in sooting laminar and turbulent diffusion flames is presented. The method is based on the two-dimensional detection of Rayleigh-scattering and laser induced incandescence (LII) combined with the measurement of the integral extinction from one single Nd-YAG laser pulse. The experimental setup of this technique (RAYLIX) employs a standard Nd-YAG laser, which requires an optical delay line or a two-pulse PIV-laser, modified for this technique. The data evaluation based on the Mie theory of scattering in the Rayleigh regime and the proportionality between the LII-signal and the soot volume fraction is given as well as an extensive error calculation. By this, a distinction is made between experimental errors from the detection system and errors arising from several assumptions from scattering theory. Main error sources are assumptions for the standard deviation of the lognormal size distribution and a constant refractive index of the soot particles. Additionally, the postulated proportionality between the LII-signal and the soot volume fraction is investigated. Applications of the RAYLIX-technique are presented including laminar and turbulent acetylene/nitrogen diffusion flames burning in air. From this, fundamental conclusions concerning soot formation and oxidation can be drawn and consequences for modelling of soot formation processes are discussed. Furthermore, laminar diffusion flames are investigated under conditions that are comparable to exhaust gas recirculation. In these flames increasing inert gas concentration decreases rates of soot formation and less soot is formed. On the other hand, increasing inert gas concentration decreases oxidation rates causing thereby higher soot emission levels. Finally, promising future applications of the RAYLIX-method are discussed such as online monitoring of soot particles in soot-producing reactors and the measurement of other nanoscaled particles.

INTRODUCTION

A number of properties of nanoparticles depend on the particle size. Often such particles are found in the exhaust gases emitted from technical devices like Diesel engines or waste incineration facilities. Therefore, the exhaust gases of those devices must be characterized with respect to particle size and number density.

Several methods for the investigation of particle sizes are available. The most important techniques are the direct imaging methods like TEM, AFM or light microscopy, in which a picture of the particles is provided and the particle radii are measured directly by image processing. These methods give much information about the particles such as the size, number, shape and the agglomeration structure. However, they have two main disadvantages: First, the particles must be sampled and second, the particles are observed at other conditions than the sampling conditions. The sampling procedure can influence the results and limits the spatial resolution.

Alternatives are optical methods, which do not image the particles directly. These techniques like light- or X-ray scattering, dynamic light scattering or laser-induced incandescence obtain information about the particles from models for the interaction of particles with radiation e.g. the Mie theory for the scattering of light. These methods allow nonintrusive in-situ measurements, which are very important in systems where small structures must be resolved, and which are influenced by a sampling step. An example for such a system is a turbulent flame.

The method presented in this paper was developed to measure primary particle number densities and primary particle radii of soot in laminar and turbulent diffusion flames. In the latter, the soot properties must be determined with high temporal resolution, to resolve the turbulent fluctuations and with high spatial resolution, because of steep gradients of soot concentrations in these flames. Thus, only methods without a sampling procedure can be applied. The primary particle radius of soot in these flames is in the range of about 3 nm to 30 nm. Therefore, the application of the RAYLIX-technique to the determination of soot properties can serve as an example for the measurement of nanoscaled particles.

DESCRIPTION OF THE LASER DIAGNOSTIC TECHNIQUE

The diagnostic technique described in this work (see Suntz et. al. (1997), Geitlinger et. al. (1998)), is based on the two-dimensional detection of Rayleigh-scattering and laser induced incandescence (LII) in combination with the detection of the integral extinction (RAYLIX). The experimental results from this method are two-dimensional fields of volume fractions, number densities and the median of the particle radius. The experimental setup of the RAYLIX-technique for measuring of soot particles in turbulent diffusion flames is shown in Fig 1. There are two possible configurations for the experiment: A setup with a standard Nd-YAG Laser and another with a slightly modified PIV-Laser.

In the standard Nd-YAG setup, one single frequency-doubled Nd-YAG-laser pulse is used for the simultaneous detection of Rayleigh-scattering and LII by means of two image intensified CCD-cameras. Scattering and LII are detected in 90° and 270° , respectively, to the direction of the laser beam.

An antireflection coated BK7-plate (G_1) splits the initial laser beam, which is polarized perpendicularly to the plane of the experiment, into a low energy ($\approx 0.1mJ$) and a high energy ($\approx 5.3mJ$) beam. The latter pulse is delayed with respect to the first for 25 ns by using an optical delay-line. The result is a sequence of two laser light pulses with different intensities, which are used to detect scattering, extinction and LII. The use of a PIV-Laser, which can emit a sequence of pulses directly, saves the use of the delay-line and, therefore, it is easier to adjust.

A Galileo-telescope (L_1+L_2) is used to form a light-sheet for both beams. The spherical lens L_2 produces a smooth focus in the vertical plane. The low energy beam is used to measure Rayleigh-scattering and extinction of the soot particles. The scattered light is imaged onto the central region of the image intensifier of CCD-camera 1. The vertical polarized component of the scattered light is extracted from the flame luminosity, fluorescence or eventually excited LII-signals by a polarizer and an interference filter (532nm/10nm). This signal is put on an absolute scale by calibrating with the known scattering cross section of nitrogen.

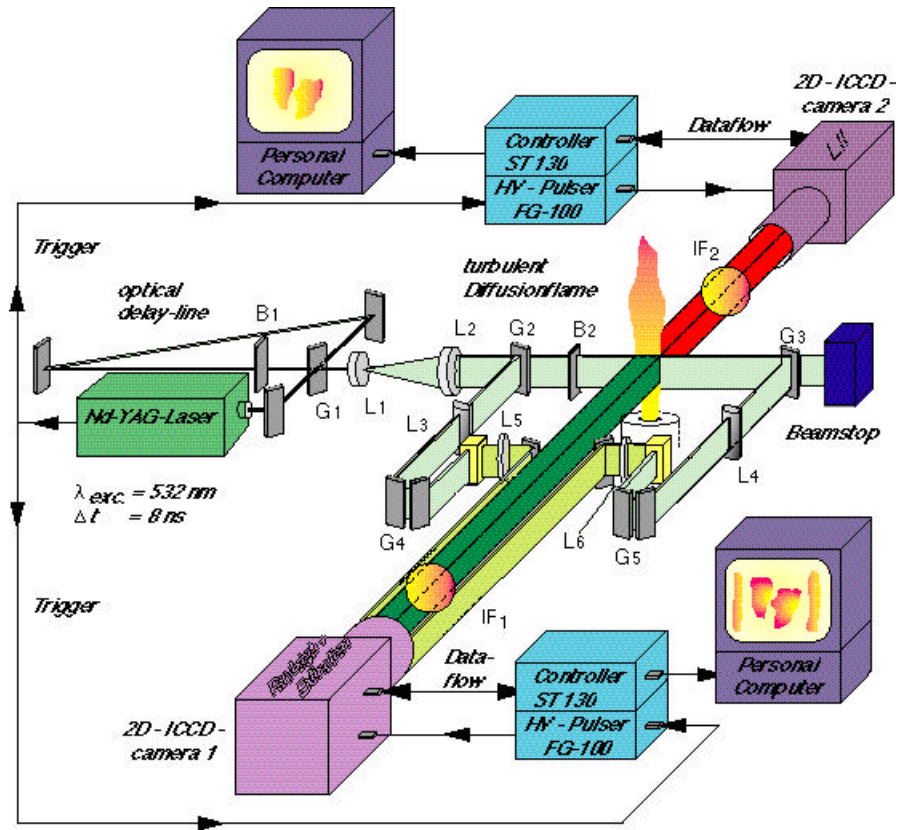


Fig. 1: Experimental setup of the RAYLIX-technique

Additionally, the profiles of the incoming and the attenuated light are measured by camera 1. The profiles are imaged onto the outer region of the image intensifier in the following way (Arnold et. al. (1997))): Two BK7-plates are inserted into the laser beam path, one in front of the flame (G_2), the other behind (G_3). Thus, the incoming as well as the attenuated light is guided into cuvettes filled with dye solution (Rhodamine 6G) by means of appropriate lenses. In front of each cuvette, additional BK7 plates are inserted in order to attenuate the intensity of the light sheet. At low intensities the fluorescence of the dye reflects the vertical intensity profiles of the laser beam. The fluorescence of the incoming and the attenuated beam are imaged onto the left and the right hand side of the scattering signal. The fluorescence of the dye solutions is measured also without a flame. So the extinction can be evaluated without the influence of the dye solution concentration or different focusing of the laser sheet. After closing camera 1, the high-energy beam passes the flame and induces the LII-signal, which is detected by camera 2. In front of camera 2 an interference filter (430nm/32nm) is used, too. This filter increases the ratio between the LII-signal and the normal (unexcited) thermal radiation due to the fact that the maximum of the Planck distribution is shifted to shorter wavelengths with increasing particle temperature. The LII signal is calibrated using the measured integral extinction to obtain absolute values of the soot volume fraction.

DATA EVALUATION

The intensity of the attenuated light beam is given by the Lambert-Beer-law:

$$I = I_o \exp\left(-\int K_{ext} dx\right) \quad (1)$$

The extinction coefficient K_{ext} can be calculated by means of the Mie-theory (see e.g. van de Hulst (1957), Kerker (1969)). For small spherical particles ($r \ll \lambda$) the Rayleigh approximation is valid and the following equation holds:

$$K_{ext} = -\frac{8\mathbf{p}^2}{I} N_v \operatorname{Im} \left(\frac{m^2 - 1}{m^2 + 2} \right) \int r^3 p(r) dr \quad (2)$$

The volume fraction of particles in an aerosole is a function of the number density and the particle size distribution $p(r)$:

$$f_v = \frac{4}{3} N_v \mathbf{p} \int r^3 p(r) dr = \frac{V_p}{V_{tot}} \quad (3)$$

Combination of equations (1), (2) and (3) leads to an equation for the averaged soot volume fraction along the extinction path:

$$\langle f_v \rangle = \frac{I \ln \left(\frac{I}{I_0} \right)}{6\mathbf{p} \operatorname{Im} \left(\frac{m^2 - 1}{m^2 + 2} \right)} \quad (4)$$

By measuring of the integral extinction the averaged soot volume fraction along an extinction path can be determined. A technique to measure local soot volume fractions is the laserinduced incandescence (LII) (see e.g. Tait and Greenhalgh (1993), Quay et. al. (1994), Vander Val and Weiland (1994), Bengtsson and Aldén (1995)). It is based on the detection of the thermal radiation of a particle, which is heated up by an intense laser pulse. A particle, which absorbs light, loses the heat through different transfer mechanisms to the surrounding gas phase. At particle temperatures below 3000 K heat conduction is the dominant process. Very high laser intensities lead to particle temperatures where soot particles emit carbon-fragments. The limit of the laser intensity for the formation of carbon clusters is about 30 MW/cm². At this point the laser intensity has little influence on the temperature of the particle. A further increase of the laser intensity accelerates the evaporation of carbon clusters and the temperature of the particles remains constant. This effect has the advantage that small fluctuations of the laser intensity do not influence the measurement.

Solutions of the mass and heat transfer equations for a soot particle in an electromagnetic field (Melton (1984)) and measurements in premixed flames show that the laserinduced thermal radiation is approximately proportional to the soot volume fraction.

Absolute values can be calculated by calibrating the relative soot volume fractions with the averaged soot volume fraction of the integral extinction. The calibration constant is given by the following equation:

$$C_{cal} = \frac{I \ln \frac{I}{I_0}}{6\mathbf{p} \operatorname{Im} \left(\frac{m^2 - 1}{m^2 + 2} \right) \int_0^r I_{LII}(x) dx} \quad (5)$$

The soot volume fraction depends on the number density and the particle size distribution according to equation (3). To calculate the median of the particle size distribution a second measurement is needed which gives a signal as a function of number density and particle size, if the particle size distribution function is known. The signal from Rayleigh scattering satisfies these demands. This signal is a function of number density and the sixth moment of the particle size distribution:

$$K_{sca} = P_{sca} / I_0 = \frac{128\mathbf{p}^5 N_v}{3I^4} \left| \frac{m^2 - 1}{m^2 + 2} \right|^2 \int r^6 p(r) dr \quad (6)$$

From the kinetics of particle coagulation and from measurements of the particle size distribution in premixed flames it is known that the particle size distribution of soot can be approximated by a lognormal distribution with a

standard deviation $\ln \mathbf{S}$ of approximately 0.34. The median of the particle radius and the number density are then given by:

$$r_m = \left(\frac{K_{sca} I^4}{32p^4 \left| \frac{m^2 - 1}{m^2 + 2} \right|^2 \exp\left(\frac{27}{2} \mathbf{S}^2\right) f_v} \right) \quad (7)$$

$$N_v = \frac{24p^3 \left| \frac{m^2 - 1}{m^2 + 2} \right|^2 f_v^2 \exp(9\mathbf{S}^2)}{I^4 K_{sca}} \quad (8)$$

DISCUSSION OF ERRORS AND PROBLEMS

There are two main error sources, viz. experimental errors and errors arising from model assumptions.

Experimental Errors

One experimental error is the induction of molecular fluorescence by the laser pulse. In general, interference from fluorescence will increase with decreasing wavelength. Therefore, the use of an infrared light source would be the best method to avoid this interference. However, the scattering cross section is inversely proportional to the 4th power of the wavelength so that a scattering signal at 532 nm (VIS) is factor 16 higher than a signal at 1064 nm (IR). Additionally, the spectral response of typical ICCD detectors is higher at 532 nm. In the visible range the main fluorescence interfering with the LII-signal in sooting flames comes from C-radicals. An appropriate detection wavelength and a delayed detection decrease this error for the LII signal to a negligible factor. The scattering signal can be separated from fluorescence by narrow interference filters and a polarizer.

In systems, where the particles attain high temperatures the black body radiation of particles which are not in the detected volume are collected by the detector. For a 0-D detector (photomultiplier) this error can be reduced significantly by a space filter. Using a 2-D detector (ICCD) a space filter cannot be applied. In this case the error can be measured in stationary systems (e.g. laminar flames) by detection without laser irradiance. In non-stationary systems (e.g. turbulent flames) this is not possible and other methods must be applied. A reduction of the contribution from the luminosity is possible by detecting LII at short wavelengths due to the shift of the maximum of the Planck distribution to shorter wavelengths with increasing particle temperature (Wien's law). The scattering signal is not influenced significantly by this radiation, if detected through a narrow filter. The error from the luminosity is estimated from experimental data of a laboratory turbulent diffusion flame, which is described in Geitlinger et. al. (1999). The flame luminosity is about 3% at positions where high soot volume fractions are detected.

The laser light is attenuated along the beam path due to extinction. This influences both the LII and the scattering signal. The LII signal can either decrease, which is the expected effect, or increase. The expected decrease in the signal strength is caused by a decrease of the particle temperature with decreasing laser intensity. At high laser fluences, which are used in an LII measurement, the particles shrink during the laser pulse. The higher the intensity the smaller the resulting particles. Small particles cool faster than large ones and, therefore, the time integrated LII signal is smaller for small particles. These facts lead to the unexpected effect of decaying signal intensity with increasing laser intensity. Figure 2 shows the typical LII signal response as a function of laser intensity. There is a decaying slope after the first maximum. To reduce the variation of the LII signal with changing laser intensity a measurement in the region of the first maximum is favourable, because the change of the signal response versus intensity is relatively small. An approximately constant LII signal can be achieved even when the laser intensity changes. The error in the LII signal is about 2.7% at an extinction of 20%, which is depicted also in figure 2.

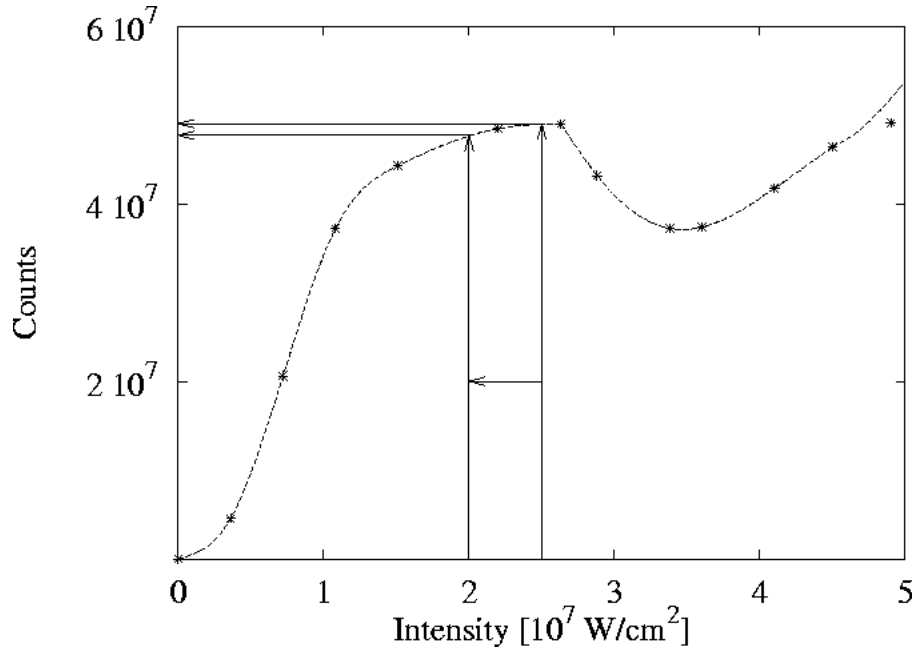


Fig. 2: Intensity of LII-signal as a function of laser intensity

The scattering signal is a linear function of the local laser intensity. Therefore, the error from the scattering signal is the same as the uncertainty in the local laser intensity. This error can be reduced significantly by calculating the local laser intensity from the soot volume fraction data measured by LII. An error calculation for the local laser intensity gives the following expression for the relative error in I as a function of the relative error in f_v :

$$\Delta I / I = \ln\left(\frac{I}{I_0}\right) \Delta f_v / f_v \quad (9)$$

If the transmission is higher than 80% this expression gives a relative error of $< 5 \%$ for I if an error of $< 20 \%$ in f_v is assumed.

In addition to the extinction along the laser beam path there is also extinction along the path from the laser sheet to the detector. This is a much more severe problem. In axisymmetric systems e.g. laminar coannular diffusion flames this effect can be calculated and corrected in the same manner as the extinction along the beam path. In non-stationary systems the particle volume fractions are not known. In this case, this error, which can roughly be estimated to one half of the measured integral extinction, must be taken into account.

Further errors connected with the detection of the signals are the nonlinearity of the ICCD detector, which is given as 1% by the manufacturer. The readout noise is negligible.

Errors from Model assumptions

Additionally, errors arise from model assumptions. The following assumptions are made when calculating volume fractions, radii and number densities of the particles:

- Particles are very small (Rayleigh regime)
- Particles are spherical
- No agglomerates
- Lognormal size distribution
- Constant refractive index
- $LII \sim f_v$

The first assumption can be released by solving the Mie theory for this problem exactly and use polynomial fits for the Mie-coefficients. In this case no assumptions are necessary. Figure 3 shows the difference between the Mie and the Rayleigh solutions of the scattering and the extinction efficiency for soot particles at a wavelength of 532 nm. For particle sizes smaller than 30 nm the error of the approximation is smaller than < 4% for the extinction efficiency and < 7% for the scattering efficiency at these conditions.

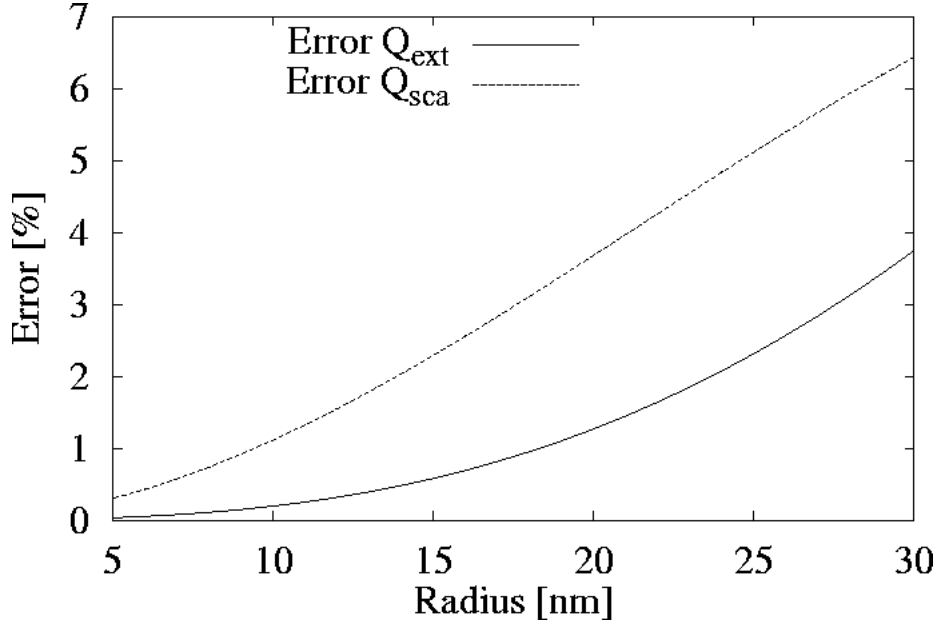


Fig. 3: Deviation between Mie and Rayleigh solution of extinction and scattering efficiency; $I = 532 \text{ nm}$

The assumption of no agglomerates is definitely not valid for soot. However, it is reasonable to assume that the primary particles act as single scatterers in the agglomerate. Jones (1979) investigated the effect of agglomeration on Q_{sca} and Q_{ext} . The error on these values is about 7 % assuming randomly oriented chains.

The main problem of the RAYLIX technique is the assumption of a lognormal size distribution with a fixed standard deviation. Lognormal size distributions fit best the size distributions in systems where particles grow mainly due to coagulation. The standard deviation of lognormal size distributions of soot in literature varies from 0.28 to 0.38. This variation will be used in the following error calculation. If the real size distribution is multimodal, e.g. due to mixing effects, the RAYLIX-technique gives biased results. A further uncertainty, which is inherent in scattering and extinction measurements, is the variation of the complex refractive index of the particles. In the case of soot the data ranges from 1.35-0.4i to 2.0-1.0i.

The previously described theoretical errors are due to the scattering and extinction part of the system. The LII signal processing is also based on the assumption that the measured signal, which is a time integration of the decay curve of the black body radiation of the laser-heated particles, is assumed to be linear correlated to the volume fraction of the particles. This assumption is based on different experimental findings (e.g. Quay et. al. (1994), Bengtsson and Aldén (1995)). The theoretical description of the LII signal has not reached a stage where all processes involved are completely understood. Current models show a deviation from the LII- f_v proportionality, which increases with increasing detection delay and gate width. It is very difficult to estimate errors here, because the error depends on many variables such as gas temperature and pressure, detection conditions, laser intensity, particle radii and concentration. From the differences between extinction and LII measurements in laminar premixed flames we estimate this error to 20% (Appel et. al. (1996)).

An error calculation gives the following two equations for the calculation of the error in the soot volume fraction:

$$\frac{\Delta C_{cal}}{C_{cal}} = \frac{1}{t} \left[\frac{\Delta I}{I} - \frac{\Delta I_0}{I_0} - t + \frac{\Delta \text{Im}\left(\frac{m^2 - 1}{m^2 + 2}\right)}{\text{Im}\left(\frac{m^2 - 1}{m^2 + 2}\right)} \right] \quad (10)$$

$$\frac{\Delta f_V}{f_V} = \frac{\Delta C_{cal}}{C_{cal}} + \frac{\Delta I_{LII}}{I_{LII}} \quad (11)$$

The error in the detected intensities ΔI_0 and ΔI when calibrating with a high number of frames (no photonic noise) are assumed as the following:

- Nonlinearity of the detector
- Digitising error 0.2%

The nonlinearity influences the error very little due to the different signs in equation (11). The following calculation assumes an extinction of 20 %.

The error in the term with the refractive index is calculated from a span of refractive indexes in a methane flame (Charampolous and Felske (1987)). The term varies from -0.28 to -0.22. This leads to a relative error of the calibration constant of the LII signal of $\pm 13\%$. The error with an exact known refractive index is much less (1.4%). Another error is the error due to the Rayleigh assumption in the extinction formula. This error increases with the radius and attains approximately 4 % at a particle radius of 30 nm. This error is neglected here, due to the fact that it can be avoided by using the correct Mie expressions.

The error in the soot volume fraction is the sum of the error in the calibration constant and the error in the LII-intensity I_{LII} . This error, which is due to the varying particle radius, is assumed to be 20 % (Appel et.al. (1996)).

$$\Delta f_V / f_V = \pm 0.13 + \pm 0.2 = \pm 0.33 \quad (12)$$

The following equation describes the error in the particle radius:

$$\frac{\Delta r_m}{r_m} = -\frac{\Delta K_{sca}}{K_{sca}} + \frac{\Delta f_V}{f_V} + 9\mathbf{S} \Delta \mathbf{S} + \frac{2}{3} \frac{\Delta \left| \frac{m^2 - 1}{m^2 + 2} \right|}{\left| \frac{m^2 - 1}{m^2 + 2} \right|} \quad (13)$$

With the variation in f_V of $\pm 33\%$, an error of 6% in K_{sca} , a variation of \mathbf{S} from 0.28 to 0.38 and a variation

from 0.33 to 0.61 for the term $\left| \frac{m^2 - 1}{m^2 + 2} \right|$ an error in r_m of ± 0.48 is calculated.

This error of 48 % represents the worst case, when the logarithm of the standard deviation \mathbf{S} is not measured in a calibration procedure at similar conditions.

The error of the particle number density is given by the following equation:

$$\Delta N_V / N_V = \frac{2 \Delta f_V}{f_V} + 18\mathbf{S} \Delta \mathbf{S} - \frac{\Delta K_{sca}}{K_{sca}} + 2 \frac{\Delta \left| \frac{m^2 - 1}{m^2 + 2} \right|}{\left| \frac{m^2 - 1}{m^2 + 2} \right|} \quad (14)$$

It can be estimated to ± 1.6 .

The error in the particle number density seems to be very high, however, one must keep in mind that the number density is changing over several orders of magnitudes.

SOME APPLICATIONS OF THE RAYLIX-TECHNIQUE

The RAYLIX-technique for two-dimensional detection of soot volume fractions, particle number densities and mean particle radii was applied to different systems: laminar and turbulent jet diffusion flames and co-flowing laminar diffusion flames. From this, basic conclusions concerning soot formation and -oxidation can be drawn by discussing the two-dimensional maps of the aforementioned soot properties.

Firstly, measurements were carried out in a laminar jet diffusion flame burning in surrounding air. The fuel was acetylene diluted by nitrogen (0.08 l/min and 0.2 l/min, respectively). 100 single shots were averaged to increase the signal/noise-ratio. In Fig. 4 radial profiles of soot volume fraction, particle number densities and mean particle radii at different heights above the burner are given. At those radial positions where the particle number density exhibits a maximum, a minimum in the particle radii appears. This indicates, that the soot formation zone is located here, where particle inception occurs by coagulation of PAH's leading to a large number of small particles. Towards lower radial distances the particle radius increases due to surface growth reactions, which also cause the somewhat shifted maximum in soot volume fraction, and coagulation. With increasing height above the burner, the distinct profiles of the left and right side are moving and, finally, are fusing together. Large particles can be observed in the centre of the flame, where coagulation processes dominate.

In Fig. 5, two-dimensional maps of soot volume fractions, particle number densities and mean particle radii as false colour plots are given for a turbulent jet diffusion flame burning in surrounding air. The fuel was 2 l/min acetylene diluted by 2 l/min nitrogen. Therefore, the Reynolds number at nozzle exit conditions is about 4000. The turbulent structure of the flame can clearly be seen from Fig. 5. There are defined structures with high particle number densities and low mean particle radii similarly to the laminar flames (see Fig. 4). The fact, that these structures are preserved in the turbulent flame gives evidence that soot formation in turbulent diffusion flames in the investigated Reynolds-regime takes place in laminar flamelets. Time scales of soot formation and, moreover, soot oxidation also, seem to be smaller than those of turbulent mixing. When modelling of soot formation in these systems, models comprising fast chemistry assumptions such as the Flamelet-model could be used calculating soot properties and species concentrations.

Exhaust gas recirculation (EGR) was simulated by investigating co-flowing laminar diffusion flames with variable composition of the oxidizer flow. The fuel was acetylene (0.1 l/min) diluted by nitrogen (0.25 l/min). The oxidizer flow (10 l/min) consisted of air diluted by carbon dioxide. This accounts for the decreasing oxygen and increasing inert gas concentration when operating with EGR. In Fig. 6 two-dimensional fields of soot volume fractions of three different flames are given. With increasing CO₂-mole fraction, soot formation seems to be delayed and a lower maximum soot volume fraction is observed. This is caused by a decreasing combustion temperature due to the higher content of inert gas, leading to a decrease in the rate of soot formation reactions. On the other hand, soot oxidation reactions are also decelerated due to the lower temperature, therefore, a higher emission level is observed at the flame tip. These findings are illustrated in Fig. 7, where axial profiles of soot volume fractions in the burner axis are given. When oxidation of soot particles dominates (after the maximum) the slope of the curves becomes less steep with increasing inert gas concentration and the curves intersect at higher heights above the burner.

OUTLOOK

The RAYLIX-technique offers a tool to measure particle sizes and particle number densities with a two-dimensional detection method. Results for laminar and turbulent diffusion flames showed the successful application of this measurement technique. In future work, RAYLIX will be applied to investigate the exhaust gas of DI-spark ignition engines and soot formation in industrial plants. Moreover, applications are possible for other nanoscaled particles like SiO₂ and metal particles (vander Wal 1998).

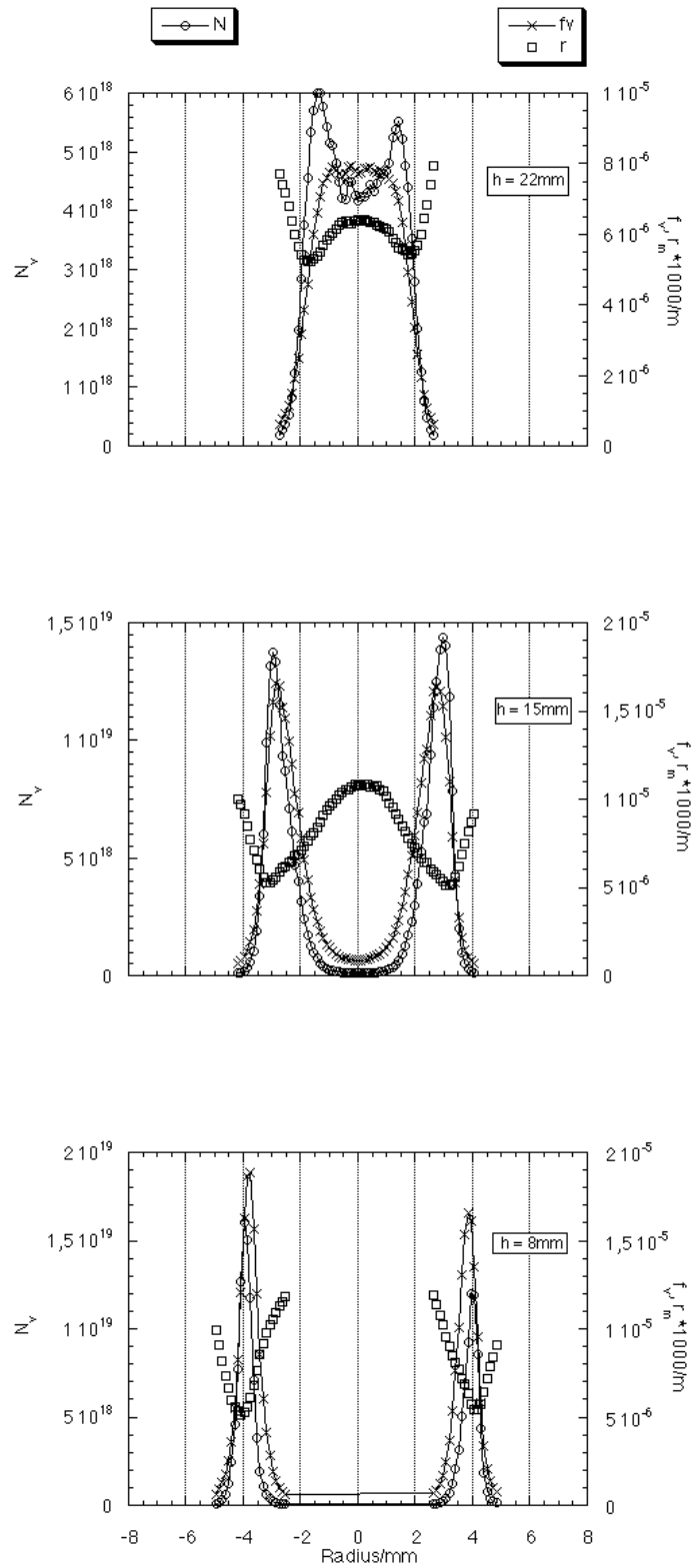


Fig. 4: Radial profiles of f_v , N_v and r_m in a laminar jet diffusion flame

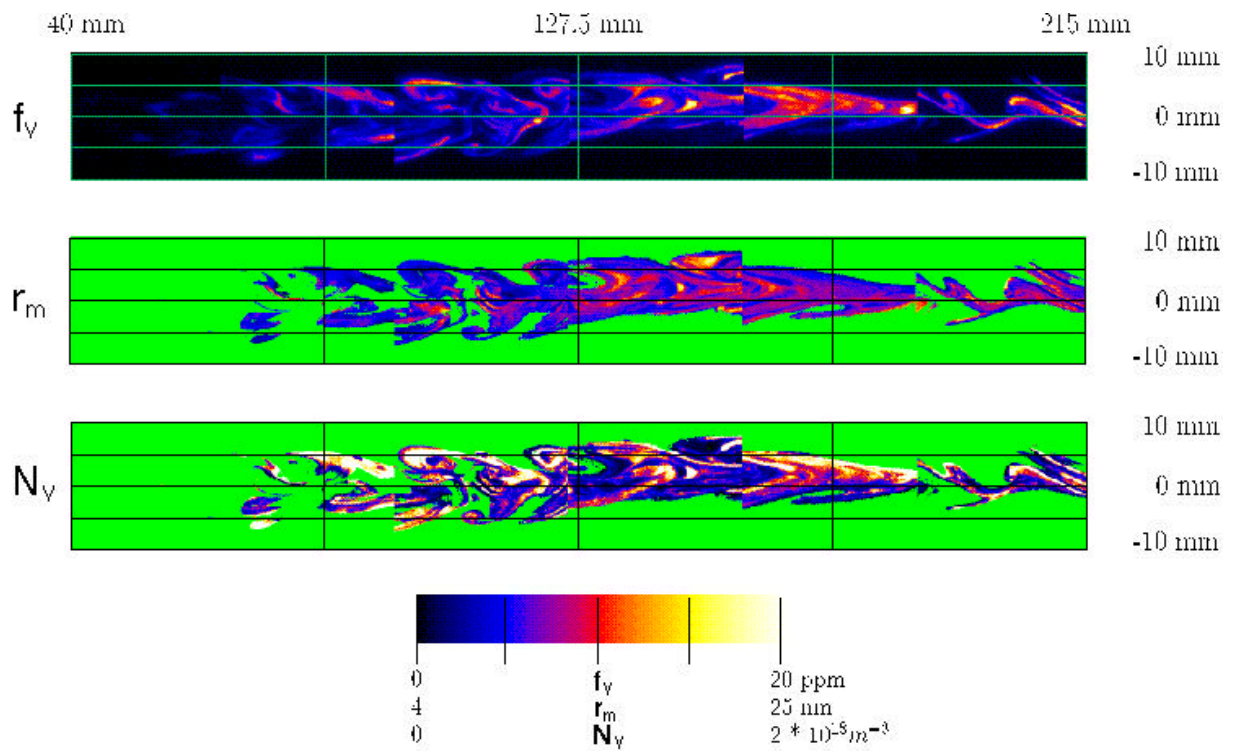


Fig. 5: Two-dimensional maps of single shots of f_v , N_v and r_m in a turbulent diffusion flame

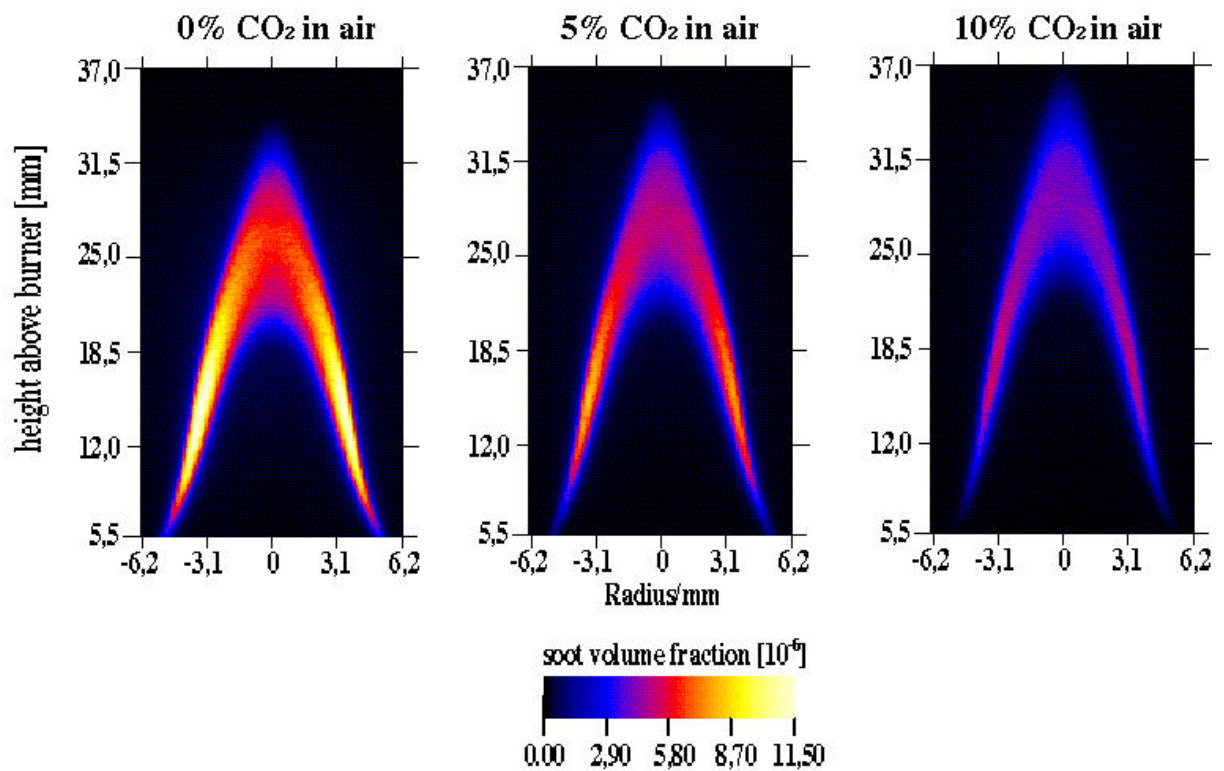


Fig. 6: Two-dimensional maps of f_v in laminar co-flowing diffusion flames with simulated EGR

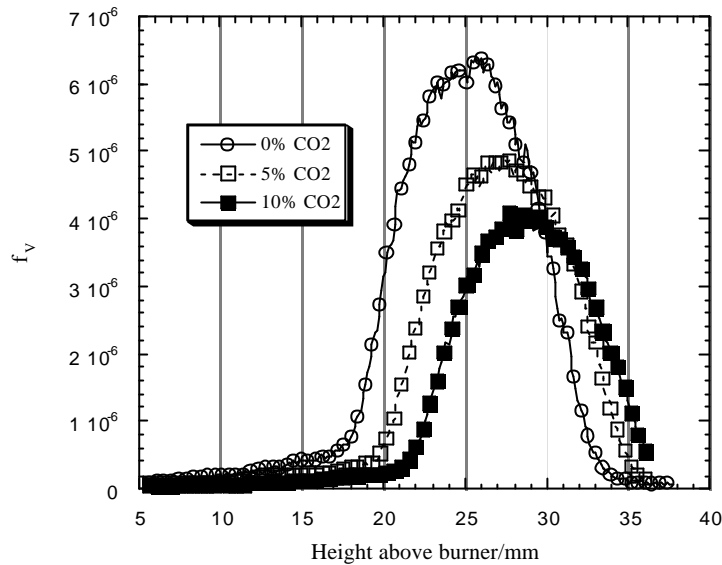


Fig.7: Axial profiles of f_v in the burner axis ($R = 0\text{mm}$) of the flames from Fig. 6

REFERENCES

- Appel, J., Jungfleisch, B., Marquardt, M., Suntz, R., and Bockhorn, H., *Proc. Combust. Inst.* 26:2387-2395 (1996)
- Arnold, A., Bombach, R., Käppeli, B., and Schlegel, A., *Appl. Phys. B* 64:579-583 (1997)
- Bengtsson, P.-E., and Aldén, M., *Appl. Phys. B* 60:51-59 (1995)
- Charalampopoulos, T. T., and Felske, J. D., *Combust. Flame* 68:283 (1987)
- Geitlinger, H., Streibel, T., Suntz, R., and Bockhorn, H., *Proc. Combust. Inst.* 27:1613-1621 (1998)
- Geitlinger, H., Streibel, T., Suntz, R., and Bockhorn, H., Fifth International Conference on Technologies and Combustion for a Clean Environment, Vol. 2, 1101-1111, The Combustion Institute, Portuguese Section, 1999
- Jones, A. R., *J. Phys. D.* 12 :1661-1672 (1979)
- Kerker, M., *The Scattering of Light and Other Electromagnetic Radiation*, Academic Press, New York, 1969
- Melton, L.A., *Appl. Optics* 23:2201-2208 (1984)
- Quay, B., Lee, T.-W., ni, T., and Santoro, R. J., *Combust. Flame* 97:384-392 (1994)
- Suntz, R., Marquardt, M., Jungfleisch, B., and Bockhorn, H., Fourth International Conference on Technologies and Combustion for a Clean Environment, Lisbon, 24.1, 1997
- Tait, N. P., and Greenhalgh, D. A., *Ber. Bunsen-Ges. Phys. Chem.* 97:1619-1625 (1993)
- Van de Hulst, H. C., *Light Scattering by Small Particles*, Wiley & Sons, New York, 1957
- Vander Wal, R. L., and Weiland, K. J., *Appl. Phys. B* 59:445 (1994)
- Vander Wal, R. L., Ticich, T. M., and West, J. R., *Appl. Optics* 38:5867-5879 (1998)